Strong suppression of positron-induced double ionization of helium at low-to-intermediate velocities

A. X. Yang, X. R. Zou, C. N. Lin, W. B. Liu, S. T. Niu, X. M. Chen, and J. X. Shao*
School of Nuclear Science and Technology, Lanzhou University, Lanzhou 730000, China
(Received 2 July 2014; published 2 February 2015)

Based on our previous work of the classical over-barrier ionization model, the single- and double-ionization cross sections of positron-helium impact are calculated. The calculation results are consistent with the experimental data. The screened Coulomb potential is used to obtain the trajectory of the positron in single-ionization process. The positron is seemed to be scattered by the rest He^+ core in double ionization. The strong Coulomb defection effect makes the double ionization to be significantly suppressed at low velocities.

DOI: 10.1103/PhysRevA.91.022701 PACS number(s): 34.80.Uv

I. INTRODUCTION

Helium ionization induced by positron has been studied widely both in experiments and theories. Fromme [1], Jacobsen [2], Moxom [3,4], Knudsen [5], and Ashley [6] had measured the single-ionization cross section of positron-helium collision from the threshold to intermediate and high energies. Charlton [7] measured the double-to-single ratio R_{21} of positron-helium impact and electron-helium impact and proposed the assumption that the difference of double ionization between the electron and proton was attributed to their opposite charge. Bluhme [8] found that positronium formation was strongly suppressed during the double-ionization process. In theory, Basu [9], Baluja [10], Zhifan [11], and Mukherjee [12] used quantum methods to study the ionization cross section of positron-helium scattering. Schultz and Olson [13] used the classical trajectory Monte Carlo (CTMC) method to calculate the single-ionization cross section of positron-helium collision at intermediate velocities. The second-order Born model was proposed by Kheifets [14] to describe the simultaneous ionization excitation and double ionization of He impacted by positron at velocity of 12 a.u. Simonovic [15] used the classical Newtonian method to calculate the double-ionization cross section of positron-helium impact near the threshold. Recently, Dey [16] calculated the fivefold-differential cross section (FDCS) for double ionization of He by positron impact at 610 eV. The second-order Born approximation was used by Dal Cappello [17] to calculate the fourfold-differential cross section (4DCS) of double ionization for helium impacted by positron at 621 eV.

In this paper, we extended our COBI model [18], which dealt with the double ionization of helium impacted by heavy ions, to the case of positron-impact ionization. Based on the picture of sequential over-barrier ionization, and taking the Coulomb deflection effect into account, the single- and double-ionization cross sections of positron-helium impact in low-to-intermediate velocities were obtained. The calculation results are consistent with available experimental data. The strong Coulomb deflection makes double ionization of positron-helium impact significantly suppressed at low velocities. Atomic units are used in the following context.

II. MODEL

In this model, based on the picture of sequential over-barrier ionization, the trajectory modifications induced by the Coulomb deflection effect are made to calculate the positron's trajectories in single and double ionization of helium. At first, we will review the COBI model to grasp the picture of sequential over-barrier ionization.

A. Proton-impacted ionization of helium

In Bohr's over-barrier (OB) [19] model and its extension COBM [20], two important internuclear distances are introduced. The first is the release distance R_r, in which the target electron will be released to the projectile side. The second is the capture distance R_C, in which the released electron will be captured. The two distances are respectively calculated as follows:

$$R_r = \frac{Z + 2\sqrt{qZ}}{I}, \tag{1}$$

$$R_C = \frac{2q}{v^2}, \tag{2}$$

where q and Z are the effective charges of projectile and target core; I is the ionization energy of target electron; v is the projectile's velocity.

For low-velocity collisions, $R_C > R_r$, indicating that all the released electrons will be captured and that no ionization takes place. For intermediate-velocity collisions, $R_C < R_r$, indicating that many of the released electrons cannot be captured. In the OB model, it is simply assumed that these electrons will go back to the target after collision. But, in fact, the released but noncaptured electron will be continuously accelerated by the approaching ion. In Sattin's work [29], the trajectory of released optical electron is calculated to get the single capture and ionization cross section of atom target near the velocities of 1 a.u.

For simplicity, our previous work of the COBI model had assumed that when the projectile enters the distance R_I, in which the kinetic energy of the released electron converted from the Stark energy is larger than its ionization energy, the electron will be ionized. R_I satisfies Eq. (3):

$$\frac{q}{R_I} \geqslant I + \frac{q}{R_r}. \tag{3}$$

*Corresponding author: shaojx@lzu.edu.cn

For the release, capture, and ionization processes are gradually implemented, the probabilities of these three processes should be considered as follows:

$$P_r = \frac{2\sqrt{R_r^2 - b^2}}{v}\frac{1}{T} = \frac{t_{\text{release}}}{T} \quad \text{when} \quad b \leqslant R_r, \tag{4}$$

$$P_C = \frac{2\sqrt{R_C^2 - b^2}}{v}\frac{1}{T} = \frac{t_{\text{capture}}}{T} \quad \text{when} \quad b \leqslant R_C, \tag{5}$$

$$P_I = P_r - P_C = \frac{t_{\text{release}} - t_{\text{capture}}}{T} \quad \text{when} \quad b \leqslant R_I, \tag{6}$$

where b is the collision parameter; $T = 2\pi n^3/Z^2$ is the orbital period of helium's $1s$ electron. From Eqs. (4)–(6), we know that the probabilities of release, capture, and ionization are the ratios of the release, capture, and ionization duration (t_{release}, t_{capture}, and $t_{\text{ionization}}$) to the orbital period T of target electron. It should be noted that all these probabilities are calculated under the linear trajectory approximation for incident proton.

It is important to distinguish the two electrons with subscripts i ($i = 1,2$) for helium target, R_{ri}, R_{Ci}, and R_{Ii} are the distances for the ith released electron. They satisfy the following equations:

$$R_{ri} = \frac{Z_i + 2\sqrt{q_i Z_i}}{I_i}, \tag{7}$$

$$R_{Ci} = \frac{2q_i}{v^2}, \tag{8}$$

$$\frac{q_i}{R_{Ii}} \geqslant I_i + \frac{q_i}{R_{ri}} \quad (i = 1,2), \tag{9}$$

where I_i is the ith ionization energy of the target electron and $I_1 = 24.6\,\text{eV}$, $I_2 = 54.4\,\text{eV}$ for two helium electrons, q_i and $Z_i = n\sqrt{2I_i}$ are the effective charges of the projectile and the target core seen by the ith target electron. The first released electron loses its screen ability to the target nucleus while it screens the incident projectile [18,20], the value of q_2 will be much smaller than that of q_1. In our previous work, the parameters of $Z_1 = 1.34$, $Z_2 = 2$ and $q_1 = 1$, $q_2 = 0.3$ are used [18,21–23] to obtain good calculation results in proton-impacted single- and double-ionization cross sections of helium.

B. Positron-impacted ionization of helium

The positron has the same charge with the proton, so the release, capture, and ionization distances of the two helium electrons should be the same as those for proton impact. However, the mass of the positron is about three orders of magnitude less than the proton, the Coulomb deflection effect on the positron's trajectory in single- and double-ionization processes should be considered in the calculation of the release, capture, and ionization probabilities for positron impact.

The single-ionization process may be approximately considered as the process that the incident positron is scattered by a screened helium atom. Thus, the well-known screened Lindhard potential is used to calculate the positron's trajectory in helium single ionization. Equation (10) is the screened Lindhard potential:

$$V_{\text{screen}}(r) = qZ_{\text{He}}\left(\frac{1}{r} - \frac{1}{(r^2 + 3a^2)^{1/2}}\right), \tag{10}$$

$$a = 0.8853/\left(Z_{\text{He}}^{2/3} + q^{2/3}\right)^{1/2}, \tag{11}$$

$$a_1 = 0.8853/\left(Z_{\text{He}}^{1/2} + q^{1/2}\right)^{2/3}, \tag{12}$$

$$a_2 = 0.8853/\left(Z_{\text{He}}^{0.3} + q^{0.3}\right), \tag{13}$$

where $Z_{\text{He}} = 2$ is the nuclear charge of Helium target; $a = 0.5504$, $a_1 = 0.4920$, and $a_2 = 0.3968$ are three commonly used screen parameters for positron-helium impact system; r is the distance between positron and target nucleus.

Figure 1(a) shows the schematic collision geometry of positron-helium collision for the first removed electron. The release duration of the first released electron is $t_{\text{release1}} = t_{\widehat{A_1D_1}} = \int_{A_1}^{D_1}\frac{1}{v_{e^+}}dl$, where v_{e^+} is the positron's velocity; the capture duration is $t_{\text{capture1}} = t_{\widehat{E_1F_1}} = \int_{E_1}^{F_1}\frac{1}{v_{e^+}}dl$ and the ionization duration is $t_{\text{ionization1}} = \int_{A_1}^{D_1}\frac{1}{v_{e^+}}dl - \int_{E_1}^{F_1}\frac{1}{v_{e^+}}dl$. $t_{\widehat{B_1C_1}} = \int_{B_1}^{C_1}\frac{1}{v_{e^+}}dl$ is used to judge whether positron can enter the distance R_{I1}. If $t_{\widehat{B_1C_1}} \leqslant 0$, the ionization will not occur. With the step-by-step numerical integration along the positron's trajectories, the values of $t_{\widehat{A_1D_1}}$, $t_{\widehat{B_1C_1}}$, $t_{\widehat{E_1F_1}}$ can be obtained. Like the calculation for the proton case [Eqs. (4)–(6)], the probabilities of release, capture, and ionization of the

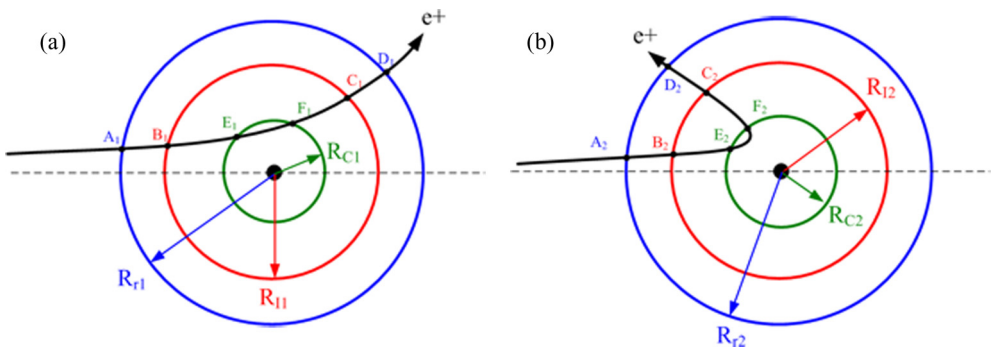

FIG. 1. (Color online) The geometry of positron-helium collision in (a) single-ionization and (b) double-ionization process.

first electron in positron-impacted helium are, respectively, calculated as

$$P_{r1}^{e^+} = \frac{t_{\text{release1}}}{T}, \tag{14}$$

$$P_{C1}^{e^+} = \frac{t_{\text{capture1}}}{T}, \tag{15}$$

$$P_{I1}^{e^+} = \frac{t_{\text{ionization1}}}{T} \quad \text{when } t_{\widehat{B_1C_1}} \neq 0. \tag{16}$$

To ensure the calculation accuracy, the variable-step 4-order Runge-Kutta method is used to solve the differential equations of position movement.

In the COBM and COBI models, the first released helium electron loses its screening capability to the target core. Thus, the approaching positron will be subjected to the strong Coulomb repulsion force coming from the rest He^+ core. The positron's trajectory during the second electron ionization process should be calculated with the unscreened Coulomb potential between positron and He^+ ion. The effective charge of the rest He^+ core is estimated to be $Z_{He^+} = 1.69$ according to the well-known Slater rules [24]. Thus, the Coulomb potential $V_{\text{unscreen}}(r)$ is used to simulate the positron's trajectory in the ionization process of the second released electron:

$$V_{\text{unscreen}}(r) = \frac{q_2 Z_{He^+}}{r}. \tag{17}$$

Figure 1(b) shows the collision geometry of positron-helium collision for the second removed electron. The release, capture, and ionization durations for the second released electron are $t_{\text{release2}} = t_{\widehat{A_2D_2}} = \int_{A_2}^{D_2} \frac{1}{v_{e^+}} dl$, $t_{\text{capture2}} = t_{\widehat{E_2F_2}} = \int_{E_2}^{F_2} \frac{1}{v_{e^+}} dl$, and $t_{\text{ionization2}} = \int_{A_2}^{D_2} \frac{1}{v_{e^+}} dl - \int_{E_2}^{F_2} \frac{1}{v_{e^+}} dl$. $t_{\widehat{B_2C_2}}$ is used to judge whether the double ionization will occur. The probabilities of release, capture, and ionization of the second released electron for positron impact are, respectively,

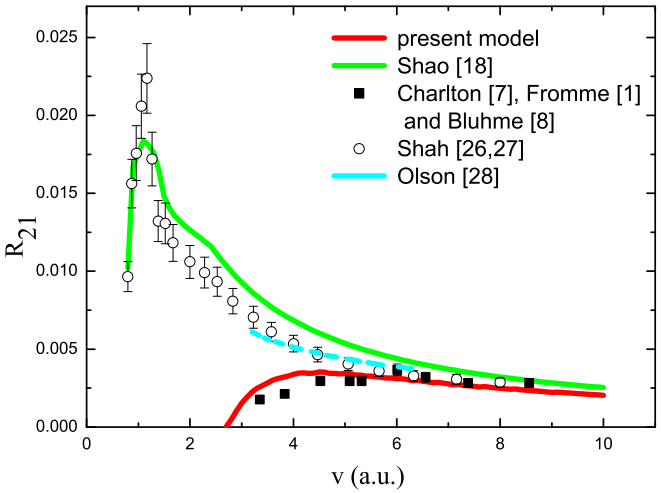

FIG. 3. (Color online) R_{21} of the proton- and positron-helium impact. The present results (red line, positron) and our previous results [18] (green line, proton). Dashed blue line represents calculation results from Ref. [28], dots are experimental data [1,7,8,26,27].

calculated as

$$P_{r2}^{e^+} = \frac{t_{\text{release2}}}{T}, \tag{18}$$

$$P_{C2}^{e^+} = \frac{t_{\text{capture2}}}{T}, \tag{19}$$

$$P_{I2}^{e^+} = \frac{t_{\text{ionization2}}}{T} \quad \text{when } t_{\widehat{B_2C_2}} \neq 0. \tag{20}$$

Now, we get the probabilities of the first released electron $P_{r1}^{e^+}$, $P_{C1}^{e^+}$, and $P_{I1}^{e^+}$, and those of the second released electron $P_{r2}^{e^+}$, $P_{C2}^{e^+}$, and $P_{I2}^{e^+}$. By using the independent event model (IEVM) [25], we can extract the two-electron probabilities from these single-electron probabilities.

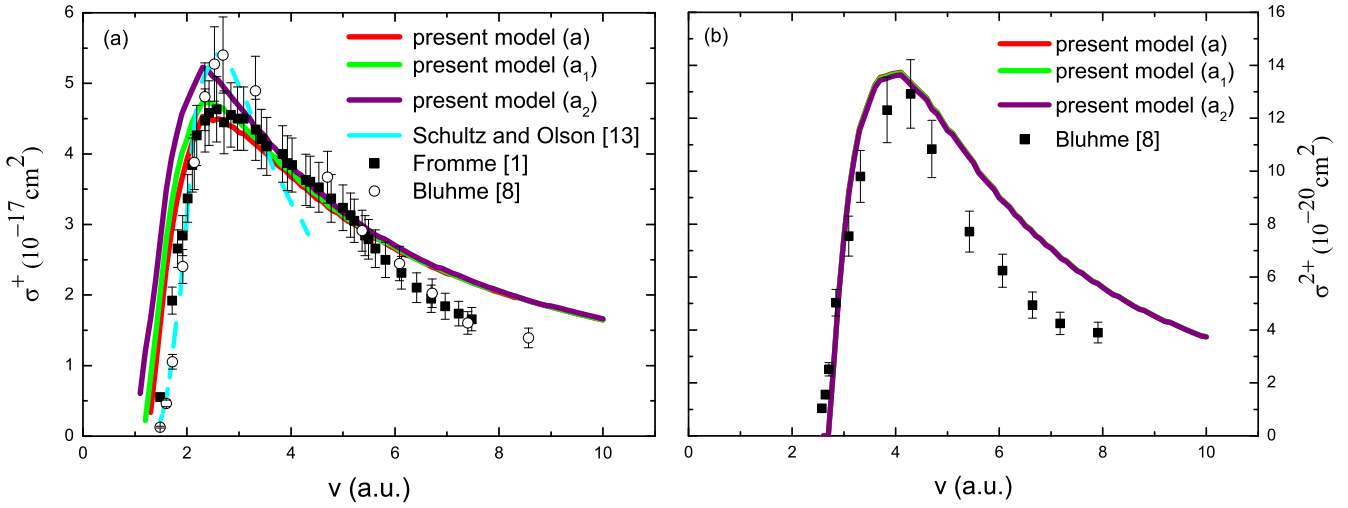

FIG. 2. (Color online) (a) Single-ionization cross section of positron-helium impact: lines are calculation results with three different screen parameters, dots are experimental data [1,8] and the dashed blue line represents Schultz and Olson's results [13]; (b) double-ionization cross section of positron-helium impact: lines are calculation results with three different screen parameters, dots are experimental data [8].

So, the single-ionization cross section is expressed as

$$\sigma^{+} = 2\pi \int P_{I1}^{e^+}\left(1 - P_{I2}^{e^+} - P_{C2}^{e^+}\right) bdb + 2\pi \int P_{I2}^{e^+}\left(1 - P_{I1}^{e^+} - P_{C1}^{e^+}\right) bdb. \quad (21)$$

The double-ionization cross section is expressed as

$$\sigma^{2+} = 2\pi \int P_{I1}^{e^+} P_{I2}^{e^+} bdb. \quad (22)$$

The double-to-single ionization ratio R_{21} is expressed as

$$R_{21} = \frac{\sigma^{2+}}{\sigma^{+}}. \quad (23)$$

III. RESULTS AND DISCUSSION

From Fig. 2(a), we can observe that our calculation results of single-ionization cross sections are not sensitive to the changes of the screen parameters. The maximum differences between them are no more than 15% and appear in the place with the maximum ionization cross section. For velocities lower than 6 a.u., calculations are well consistent with experimental data. However, for higher velocities, calculation results are somehow larger than experimental data. Calculations by Schultz and Olson [13] are well consistent with experimental data for velocities lower than 3 a.u. [8]. But, for the higher velocity, their results fall off more rapidly than the experimental data.

Calculation results and experimental data of positron-induced double-ionization cross sections of helium are plotted in Fig. 2(b). For velocities lower than 5 a.u., calculations are in good agreement with experimental data. The model and the experimental data both show that double ionization reaches its maximum at the velocity of 4 a.u. and lags behind single ionization at the velocity of 2–2.5 a.u. When the positron's

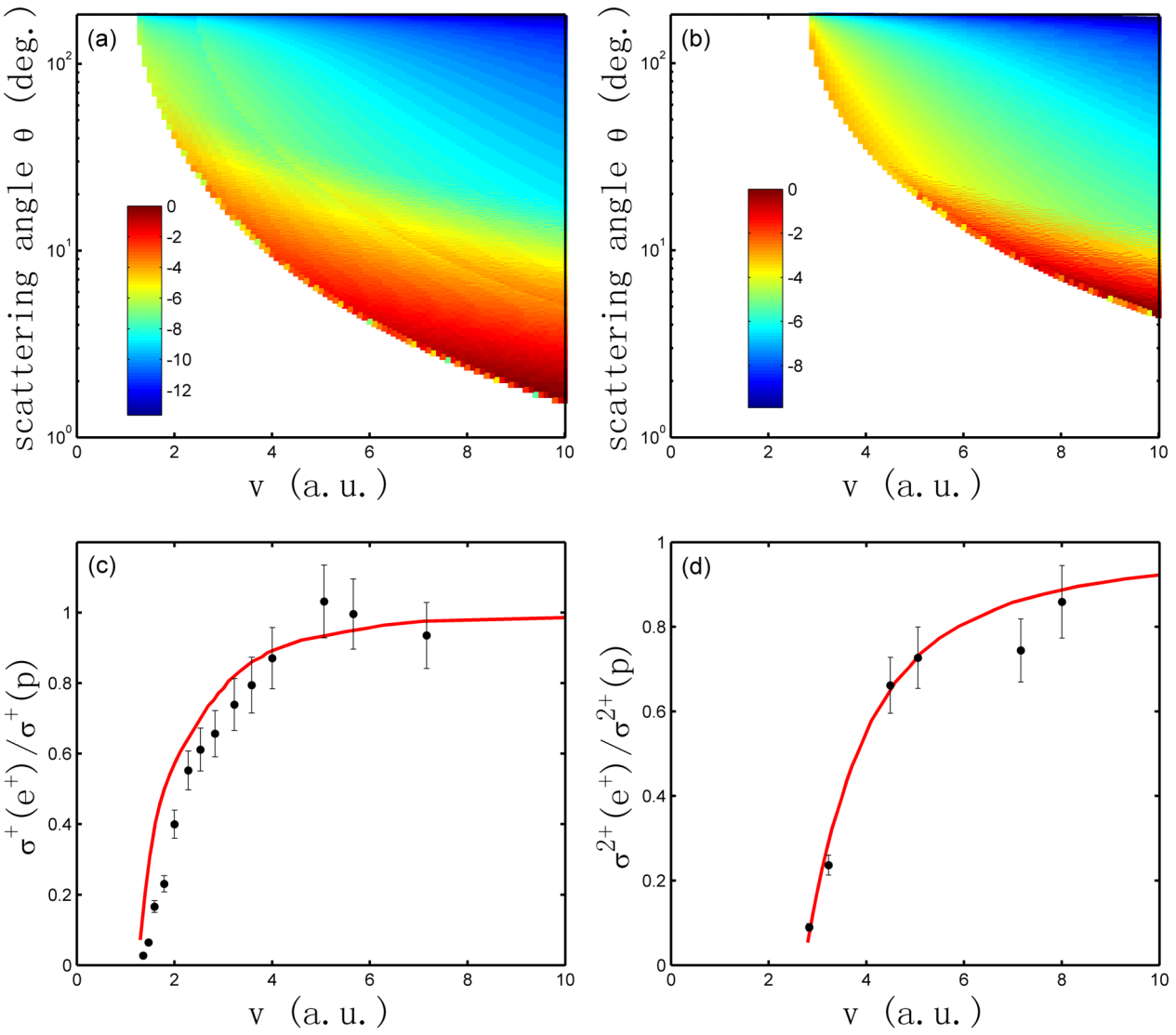

FIG. 4. (Color online) The normalized scattering probability $I(v,\theta)$ after (a) the single ionization and (b) the double ionization had occurred, and the positron is scattered to the angle of θ. Color dots represent the calculation results of $\ln[I(v,\theta)]$. Cross-section ratios of (c) single ionization and (d) double ionization of helium by positron (e^+) and proton (p) impact. Red line is our model results and dots are experimental data derived from Refs. [1,8,26].

velocity is higher than 5 a.u., the calculations are 30% larger than experimental data.

In the low-to-intermediate velocity range ($v \leqslant 5$), target electrons have enough time to pass through the Coulomb barrier. Therefore, for velocities lower than 5 a.u., the over-barrier ionization process is considered to be the main ionization mechanism. For velocities from 2 to 5 a.u., the release probability decreases as v^{-1} [22,23]. Therefore, the ionization cross section will decline slowly with v [22,23]. For higher velocities larger than 5 a.u., the release probability is too small to let the over-barrier ionization mechanism to be dominant. At this moment, violent binary encounters between projectile and target electrons start to play an important role. Violent encounters make the single- and double-ionization cross section decrease with v as v^{-2} and v^{-4} [30], respectively. Such type of decreasing rate is more rapid than that of the over-barrier ionization cross section. Therefore, the COBI model which considers the over-barrier ionization, but neglects the binary encounters, will be good at low-to-intermediate velocities and be somehow limited for higher velocities. This is the main reason that the calculations, both for the proton [18] and positron, are in quantitative agreement with experimental data obtained when the velocity is less than 5 a.u., and only qualitative agreement is obtained when the velocity is larger than 5 a.u.

The double-to-single ionization cross-section ratio R_{21} of proton- and positron-helium impact are shown in Fig. 3. The model results of proton and positron are in good agreement with experimental data, respectively. At lower velocities, significant differences are observed between proton and positron. The maximum value of R_{21} of proton (0.023) is reached near 1.2 a.u., while almost no double ionization occurs until the positron's velocity gets close to 3 a.u. The maximum value of R_{21} for the positron is only 0.003, which is much smaller than that of the proton. For higher velocities, the results of the positron gradually coincide with that of the proton. Figure 3 indicates that when the velocity is less than 4 a.u., double ionization by positron impact is strongly suppressed. When the velocity of the positron is increased to 6 a.u., the suppression effect is gradually weakened and the ratio R_{21} of the positron is basically the same to that of the proton.

To understand deeply the strong suppression to the positron-induced double ionization of helium, we calculated the scattering probabilities that the positron is scattered to a certain angle of θ after the single or double ionization occurred. As shown in Fig. 4(a), when the velocity is lower than 2 a.u., positrons are scattered to large angles of about 50° when the single ionization occurs. At the same velocity, as shown in Fig. 4(c), the positron-induced cross section is only 20% of that of the proton. When the velocity increases to 3–4 a.u., the majority of positrons which induce single ionization are scattered in the angles within 10°–20° and Coulomb deflection effect is weakened. In the meantime, the cross section of the positron is 80%–90% of that of the proton. For velocities larger than 6 a.u., the positrons which induce single ionization are scattered within the angle of 1°–5° and their trajectories are basically close to a straight line. The cross section of the positron is basically the same to that of the proton.

As shown in Fig. 4(b), it is obvious that Coulomb deflection effect applied on positron in double ionization is much stronger than that in single-ionization process. Until the velocity of the positron is close to 3 a.u., positrons cannot induce double ionization. Moreover, positrons are back-scattered in the large angle above 90°. In Fig. 4(d), the double-ionization cross section of the positron is just about 10% of that of the proton at 3 a.u. When the velocity is close to 4 a.u., the Coulomb deflection effect is still strong and the positrons which induce double ionization are scattered to the angles between 40°–60°. Moreover, the double-ionization cross section of the positron is still less than 50% of that of the proton. When the velocity is close to 6 a.u., the scattering angle of the positron which induces double ionization is within 10°–20° and the double-ionization cross section of the positron increases to 80% of that of the proton. For velocities larger than 8 a.u., the scattering angle of the positron-induced double ionization is less than 5° and the trajectories are close to a straight line. Now, the double-ionization cross section of the positron is 90% of that of the proton, and the positron and proton start to show basically consistent results.

IV. CONCLUSION

Based on the COBI model, we calculate the single- and double-ionization cross sections of positron-helium impact at low-to-intermediate velocities. Our model results are well consistent with experimental data. This indicates that the idea of sequential over-barrier ionization is applicable to describe positron collision. The positron is scattered by a screened helium atom in single ionization and scattered by an unscreened He^+ core in double ionization. The extremely strong Coulomb repulsion to the positron in double ionization is the main reason for the significant suppression of positron-induced double ionization at low velocities.

ACKNOWLEDGMENT

This work was supported by the National Natural Science Foundation of China, Grants No. 11174116 and No. 11175075.

[1] D. Fromme, G. Kruse, W. Raith, and G. Sinapius, Phys. Rev. Lett. **57**, 3031 (1986).

[2] F. M. Jacobsen, N. P. Frandsen, H. Knudsen, U. Mikkelsen, and D. M. Schrader, J. Phys. B: At., Mol. Opt. Phys. **28**, 4691 (1995).

[3] J. Moxom, D. M. Schrader, G. Laricchia, Jun Xu, and L. D. Hulett, Phys. Rev. A **60**, 2940 (1999).

[4] J. Moxom, G. Laricchia, and M. Charlton, J. Phys. B: At., Mol. Opt. Phys. **28**, 1331 (1995).

[5] H. Knudsen, L. Brun-Nielsen, M. Charlton, and M. R. Poulsen, J. Phys. B: At., Mol. Opt. Phys. **23**, 3955 (1990).

[6] P. Ashley, J. Moxom, and G. Laricchia, Phys. Rev. Lett. **77**, 1250 (1996).

[7] M. Charlton, L. H. Andersen, L. Brun-Nielsen, B. I. Deutch, P. Hvelplund, F. M. Jacobsen, H. Knudsen, G. Laricchia, M. R. Poulsen, and J. O. Pedersen, J. Phys. B: At., Mol. Opt. Phys. **21**, L545 (1988).
[8] H. Bluhme, H. Knudsen, J. P. Merrison, and M. R. Poulsen, Phys. Rev. Lett. **81**, 73 (1998).
[9] M. Basu, P. S. Mazumdar, and A. S. Ghosh, J. Phys. B: At., Mol. Opt. Phys. **18**, 369 (1985).
[10] K. L. Baluja and Ashok Jain, Phys. Rev. A **46**, 1279 (1992).
[11] Zhifan Chen and A. Z. Msezane, Phys. Rev. A **49**, 1752 (1994).
[12] K. K. Mukherjee, Phys. Rev. A **39**, 1756 (1989).
[13] D. R. Schultz and R. E. Olson, Phys. Rev. A **38**, 1866 (1988).
[14] A. S. Kheifets, Phys. Rev. A **69**, 032712 (2004).
[15] N. Simonovic, D. Lukic, and P. Grujic, J. Phys. B: At., Mol. Opt. Phys. **38**, 3147 (2005).
[16] Ritu Dey, A. C. Roy, and C. Dal. Cappello, J. Phys. B: At., Mol. Opt. Phys. **39**, 955 (2006).
[17] C. Dal. Cappello, A. Haddadou, F. Menas, and A. C. Roy, J. Phys. B: At., Mol. Opt. Phys. **44**, 015204 (2011).
[18] J. X. Shao, X. M. Chen, Z. Y. Liu, R. Qi, and X. R. Zou, Phys. Rev. A **77**, 042711 (2008).
[19] N. Bohr and J. Lindhard, K. Dan. Vidensk. Selsk. Mat. Fys. Medd. **28**, 7 (1954).
[20] A. Barany, G. Astner, H. Cederquist, H. Danared, S. Huldt, P. Hvelplund, A. Johnson, H. Knudsen, L. Liljeby, and K. G. Rensfelt, Nucl. Instrum. Methods, Phys. Res. Sec. B **9**, 397 (1985).
[21] J. X. Shao, X. M. Chen, X. R. Zou, X. A. Wang, and F. J. Lou, Phys. Rev. A **78**, 042701 (2008).
[22] J. X. Shao, X. R. Zou, X. M. Chen, C. L. Zhou, and X. Y. Qiu, Phys. Rev. A **83**, 022710 (2011).
[23] S. Y. Wang, Y. R. An, A. X. Yang, X. T. Kong, X. M. Chen, and J. X. Shao, Phys. Rev. A **89**, 054701 (2014).
[24] J. C. Slater, Phys. Rev. **36**, 57 (1930).
[25] J. Bradley, R. J. S. Lee, M. McCartney, and D. S. F. Crothers, J. Phys. B: At., Mol. Opt. Phys. **37**, 3723 (2004).
[26] M. B. Shah and H. B. Gilbody, J. Phys. B: At., Mol. Opt. Phys. **18**, 899 (1985).
[27] M. B. Shah, P. McCallion, and H. B. Gilbody, J. Phys. B: At., Mol. Opt. Phys. **22**, 3037 (1989).
[28] R. E. Olson, Phys. Rev. A **36**, 1519 (1987).
[29] F. Sattin, Phys. Rev. A **62**, 042711 (2000).
[30] H. Berg, J.Ullrich, E. Bernstein, M. Unverzagt, L. Spielberget, J. Euler, D. Schardt, O. Jagutzki, H. Schmidt-Bocking, R. Mann, P. H. Mokler, S. Hagmann, and P. D. Fainstein, J. Phys. B: At., Mol. Opt. Phys. **25**, 3655 (1992).